POLITECNICO DI TORINO
Repository ISTITUZIONALE

Photopolymerization of maleimide perfluoropolyalkylethers without a photoinitiator

Original
Photopolymerization of maleimide perfluoropolyalkylethers without a photoinitiator / Bonneaud, C., Burgess, J.M., Bongiovanni, R., Joly-Duhamel, C., Friesen, C.M.. - In: JOURNAL OF POLYMER SCIENCE. PART A, POLYMER CHEMISTRY. - ISSN 0887-624X. - STAMPA. - 57:6(2019), pp. 699-707. [10.1002/pola.29311]

Availability:
This version is available at: 11583/2726259 since: 2019-02-25T14:17:17Z

Publisher:
John Wiley and Sons Inc.

Published
DOI:10.1002/pola.29311

Terms of use:

This article is made available under terms and conditions as specified in the corresponding bibliographic description in the repository

Publisher copyright
Wiley preprint/submitted version

This is the pre-peer reviewed version of the [above quoted article], which has been published in final form at http://dx.doi.org/10.1002/pola.29311.This article may be used for non-commercial purposes in accordance with Wiley Terms and Conditions for Use of Self-Archived Versions..

(Article begins on next page)

16 November 2026

Photopolymerization of Maleimide Perfluoropolyalkylethers without a Photoinitiator

Céline Bonneaud[1], Julia M. Burgess[2], Roberta Bongiovanni[3], Christine Joly-Duhamel[1]* and Chadron M. Friesen[2]*

[1]Ingénierie et Architectures Macromoléculaires, Institut Charles Gerhardt, Ecole Nationale Supérieure de Chimie de Montpellier (UMR5253-CNRS), 8, rue de l'Ecole Normale, 34296 Montpellier Cedex 5, France ;
[2]Trinity Western University, Department of Chemistry, 7600 Glover Road, Langley, British Columbia V2Y 1Y1, Canada;
[3] Politecnico di Torino, Department of Applied Science &Technology, c.Duca degli Abruzzi 24, 10129 Torino, Italy

Correspondence to: Chadron M. Friesen (E-mail: chad.friesen@twu.ca)

((Additional Supporting Information may be found in the online version of this article. Copies of ^{1}H and ^{13}C spectra for compounds **1a-b**, **2b-c**, ^{19}F, IR, GC-MS, TGA and DSC spectra for **3b-c**, **4a-c** and MALDI-TOF for **4a-c**. IR spectra for the kinetics of photopolymerization.))

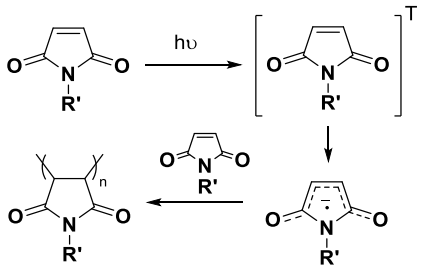
ABSTRACT

Perfluoropolyalkylethers derived from hexafluoropropylene oxide were functionalized with maleimide groups. Irradiated by UV-light, the new maleimide macromonomers demonstrated very fast polymerization kinetics with a curing time as fast as 8 seconds. The effect on photopolymerization of different features such as the molecular weight of the fluorinated chain and the chain length of the hydrogenated spacer were studied, as well as the influence of the type of photoinitiator and the presence of air. Thermal and surface properties of the UV-cured polymers were examined and were typical to fluoropolymers in view of water-oil repellent coatings.

KEYWORDS: perfluoropolyalkylethers, photopolymerization, maleimides, omniphobicity

INTRODUCTION

Photopolymerization is a green process: it occurs fast, without solvent, at room temperature and does not require a huge amount of energy.[1] Commonly, photopolymerized systems are constituted of (meth)acrylates or thiol-enes. Maleimides are alternative systems which polymerize almost as fast as acrylates but do not require a photoinitiator. Indeed, maleimides can initiate the polymerization on their own as displayed in Scheme 1. The mechanism of initiation was found to be an electron transfer which provides a radical anion which was supported by Fourier Transform-Electron Paramagnetic Resonance (FT-EPR) and by flash laser photolysis.[2,3] Thus, maleimides can homopolymerize without a photoinitiator[4] as the presence of photoinitiator can lead to their leaching or their hard removal if used in excess. Moreover, maleices can serve as photoinitiators for different types of unsaturated resins (acrylate, vinyl ether, epoxy).[5,6]



Scheme 1: Homopolymerization of maleimides by radical mechanism

Various types of maleimides were tested under UV-light such as poly(propylene glycol)-maleimides[4] or silicon-maleimides[7,8] and demonstrated the high ability of polymerization of the maleimides even in presence of long chains.

Maleimides have been found to be very useful in variety of polymer systems from "click" chemistry, self-healing polymers to thermoset polymers with high temperature stability.[9] However, the body of work on fluorinated maleimides or fluorinated moieties attached to maleimides is minimal. Barrales-Rienda et al.[10] reported in 1977 the first synthesis of fluorine-containing maleimides and their thermal polymerization using 2,2'-azobisisobutyronitrile (AIBN).[11] Much later, Mokhtar et al.[12] synthesized another maleimide, 4-(4-trifluoromethyl)phenoxy *N*-phenyl-maleimide (FPMI) which was also polymerized using AIBN. Maleimides containing pentafluoro and trifluoro groups on aromatics were copolymerized with vinyl ethers by Hendlinger et al.[13] whereas Jain et al.[14] copolymerized N-(4-fluoro phenyl) maleimide with methyl methacrylate (MMA). Daukiya et al.[15] showed the use of N-(3,4-trifluoro phenyl) maleimide with highly nonreactive graphene. Moving from single fluorines or CF_3-groups, fluorinated oligomers with maleimides was first reported by Beaune et al with C_6F_{13} chains.[16] Boutevin et al.[17] also demonstrated that maleimide-containing C_6F_{13} moieties can also be grafted onto high density polyethylene (HDPE). Few examples of fluorinated telechelic bis(maleimides) can be found having as spacers a perfluoroalkyl chain[18] or fluorinated aromatics[19] or even difluoromaleimides as telechelic end groups.[20] Lastly, maleimides have found to be useful in medical applications for radiolabeling. For example, *N*-(*p*-[18F]fluorophenyl)maleimide is used to label monoclonal antibodies.[21] Various maleimide-based compounds were exploited as reagents for protein, peptide and lipids labeling with thiol functions[22–24] and thus used in positron emission tomography (PET) imaging.[25,26]

In this study, we synthesized new maleimides characterized by perfluoropolyalkylether (PFPAE) chains, based on hexafluoropropyleneoxide (HFPO) unit -$OCF(CF_3)CF_2O$-. The synthesized monomers have a general structure R_h-R_f where R_f = $CF_3CF_2CF_2O(CF(CF_3)CF_2O)_n$ $CF(CF_3)$– with n = 5.5 and 10 and R_h = -$(CH_2)_m(CO)OCH_2$- with m = 3, 5, 10. The new monomers were photopolymerized to obtain new polymeric materials with promising performances due to the fluorinated chains. Notably, PFPAE polymers which contain ether units such as –(CF_2O)–, –(CF_2CF_2O)–, –$(CF_2CF_2CF_2O)$– and –$(CF(CF_3)CF_2O)$– are known to demonstrate excellent chemical and thermal inertness with low surface energy. They are not crystalline and are stable from -100 °C and 400 °C in the liquid state.[27] Moreover, they are attractive for use since they are non-toxic fluoropolymers and therefore can be employed in biomedical applications.[28–30]
The influence of the molecular weight of the fluorinated chain, the hydrogenated spacer length as well as the presence of air and photoinitiator on the photopolymerization process were studied.

EXPERIMENTAL

Materials

Glacial acetic acid, 11-maleimidoundecanoïc acid, 6-aminocaproic acid, 4-aminobutyric acid, maleic anhydride, thionyl chloride, triethylamine, dicyclohexylcarbodiimide, dimethylamino pyridine, 2-hydroxy-2-methylpropiophenone (Darocur 1173), diphenyl(2,4,6-trimethylbenzoyl)phosphine oxide (TPO), phenylbis(2,4,6-trimethylbenzoyl)phosphine oxide (BAPO), dichloromethane, hexadecane and deuterated solvents (DMSO-*d6*, $CDCl_3$ and C_6D_6) were purchased from Sigma Aldrich and used as received except if stated below. 1,1,1,3,3-pentafluorobutane was purchased from Alfa Aesar. The 1250 g/mol oligo(HFPO) methylene alcohol was prepared from Krytox® acyl fluoride. The 1250 g/mol Krytox® acyl fluoride and 2000

g/mol Krytox® methylene alcohol were kindly provided by the Chemours Company. Triethylamine, hexadecane and dichloromethane were dried for 48 h over preconditioned 3Å molecular sieves (20 % w/v). Thionyl chloride was previously distilled before use.

Methods

Photopolymerization by Fourier-Transform (FT) – Real Time Infrared Spectroscopy (RTIR): Real-time Infrared Spectroscopy and photopolymerization kinetics were performed on a Thermo Scientific Nicolet 6700 FTIR apparatus by using OMNIC software. A mercury lamp (OmniCure S2000) was used as UV-light source and OmniCure R2000 Radiometer was used to control the light output. A radiometer from Solatell provided a real light intensity on the sample of 10 mW cm^{-2}. A polypropylene film (6 µm) was used as air protector. The sample was irradiated during 300 s at least. Four repeats were made for each experiment. No photoinitiator was added except if specified. The conversion rate calculations were made by following the disappearance of the band at 826 cm^{-1} corresponding to the maleimide. They were calculated using the univariate method ($\tau = (1-(A/A_0))*100$). The peak deconvolution method was used to confirm the quantitative conversion. When required, an UV production curing unit Fusion UV F300S equipped with a microwave lamp (linear power output of 120 W cm^{-1}) was utilised. The sample was placed on a LC6B Bench top conveyor and passed repeatedly under the UV lamp at a speed of travel belt of 1 m min^{-1}.

Gas Chromatography (GC) Mass Spectrometry (MS): An Agilent Technologies 6890N GC was coupled with an Agilent Technologies 7638B series injector and Agilent Technologies 5975B inert mass spectrometer (MSD) was employed with electron impact (EI) as the mode of ionization. The GC was equipped with a Zebron ZB-5ms column, 30 m x 0.18 mm id, 0.18 µm df. The detector and the injector temperatures were 200 °C and 280 °C, respectively. The temperature program started from 50 °C with a 2 min hold, then the heating rate was 25 °C min^{-1} until reaching 250 °C and holding at 250 °C for 2 min. The total pressure 108 kPa, total flow was 25.9 mL min^{-1}, column flow 0.74 mL min^{-1}, purge flow 3 mL min^{-1}, linear velocity 38 2 cm s^{-1}, and a split injection of 30:1. The sample was previously diluted in methoxyperfluorobutane (3M's Novec™ HFE-7100) in a GC vial.

Nuclear Magnetic Resonance (NMR) spectroscopy: NMR spectra were recorded on a Bruker AVANCE III 400MHz spectrometer instruments using TopSpin 3.5 operating at 400.13 (^{1}H), 376.46 (^{19}F), 100.62 (^{13}C) MHz at room temperature except if specified. $CDCl_3$ and C_6D_6 capillaries were used as internal references. The letters s, d, t, q, quint, sext and spt stand for singlet, doublet, triplet, quartet, quintuplet, sextet and septuplet, respectively.

Matrix assisted laser desorption ionization time-of-flight mass spectrometry (MALDI–TOF–MS): The homologue distributions of the products were determined with a Bruker AutoflexTM *MALDI–TOF:* spectrometer equipped with a 1 kHz smartbeam-II laser and reflector in positive ionization. For sample preparation, a 1 drop sample of poly(HFPO) was added to a 1 mL solution of 50:50 1 % LiCl in MeOH and 2 % perfluorocinnamic acid dissolved in 50:50 MeOH:Methoxynonafluorobutane (3 M HFE-7100). A 1 µL solution was then pipetted on to a ground steel plate, dried, and irradiated for a minimum of 5000 shots.

Thermogravimetric analyses (TGA): The degradation temperatures were determined with a NETZSCH TG209F1 at a heating rate of 20 °C min^{-1} or 10 °C min^{-1}. Approximately 10 mg of the sample were placed in an alumina crucible and heated from room temperature to 600 °C under inert atmosphere or air (40 mL min^{-1}). To analyze the evolved gases, the instrument is coupled with a FT-IR PERSEUS Bruker heated at 200 °C and the obtained spectra are given between 4000 and 600 cm^{-1}.

Differential scanning calorimetry (DSC): The glass transition temperatures were determined with a NETZSCH DSC200F3 calorimeter. Constant calibration was performed using indium, *n*-octadecane and *n*-octane standards. 10-15 mg were placed in pierced aluminum pans and the thermal properties were recorded between -150 °C and 100 °C at 20 °C min^{-1}. Nitrogen was used as the purge gas.

Contact angle measurements: The hydrophobicity and oleophobicity were determined thanks to a contact angle system OCA20 coupled with a CCD-camera from DataPhysics Instrument using the software SCA20 4.1. The measurements were made in air at room temperature by the sessile drop technique with distilled water or previously dried hexadecane. Three repeats were made on three different samples previously spin-coated (1 min – 2000 rpm) on glass slides thanks to Spincoat G3-8 from Specialty Coating Systems and irradiated thanks to a UV bench conveyor. Their difference in the average value was no more than 3°.

Syntheses

Synthesis of 4-maleimidobutyric acid and 6-maleimidohexanoic acid (1a-b)

To a solution of maleic anhydride (2 g) in glacial acetic acid (15 mL), the corresponding amino acid was added (1 eq). The mixture was heated to reflux during 3 h. The solvent AcOH was evaporated via rotary evaporation by using toluene as azeotropic cosolvent. The crude material was extracted by using D.I. water (pH~4) and EtOAc. The aqueous phase was washed two times with EtOAc. The organic phases were combined, dried with $MgSO_4$ and concentrated under vacuum to afford an orange oil. After drying in vacuum oven, the orange solids were washed with iced D.I. water (pH~4) and dried in vacuum oven (70 °C) overnight to provide a whitish powder.

4-maleimidobutyric acid **1a** (yield=27 %): ^{1}H NMR (400 MHz, $CDCl_3$, δ): 1.92 (quint, -C**H$_2$**-, 2H), 2.35 (t, -C**H$_2$**COOH, 2H, $^3J_{H-H}$ = 7.3 Hz), 3.52 (*t,* -NC**H$_2$**-, 2H, $^3J_{H-H}$ = 6.9 Hz), 6.70 (*s,* -C**H**=C**H**-, 2H) ^{13}C NMR (101 MHz, $CDCl_3$, δ): 23.7 (-**C**H$_2$-), 31.1 (-**C**H$_2$COOH), 37.1 (-N**C**H$_2$-), 134.3 (-**C**H=**C**H-), 170.9 (-N(**C**O)-), 177.0 (-**C**OOH)

6-maleimidohexanoïc acid **1b** (yield=35 %): ^{1}H NMR (400 MHz, $CDCl_3$, δ): 1.3-1.37 (m, -C**H$_2$**-, 2H), 1.56-1.70 (m, -C**H$_2$**-, 4H), 2.35 (t, $^3J_{H-H}$ = 7.6 Hz, -C**H$_2$**COOH, 2H), 3.52 (t, $^3J_{H-H}$ = 7.3 Hz, -NC**H$_2$**-, 2H), 6.70 (*s,* -C**H**=C**H**-, 2H), 10.97 (*s,* -COO**H**, 1H) ^{13}C NMR (101 MHz, $CDCl_3$, δ): δ = 24.1 (*s*, -**C**H$_2$CH$_2$COOH-), 26.1 (*s*, -NCH$_2$CH$_2$**C**H$_2$-), 28.2 (*s*, -NCH$_2$**C**H$_2$-), 33.8 (*s,* -**C**H$_2$COOH-), 37.6 (*s,* -N**C**H$_2$-, 1C), 134.1 (*s*, -CO**C**H=**C**H-), 170.9 (*s,* -**C**ON-), 179.7 (*s,* -CH$_2$**C**OOH).

Synthesis of the acid chlorides (2b-c)

To a solution of the corresponding maleimido acid in dry DCM, 1.5 eq of triethylamine was added with 2 eq of thionyl chloride. The solution was heated at 50 °C for 3 h. The volatile compounds were removed under reduced pressure. The products were recovered quantitatively (yield>99 %) as orange-brown solids.

6-maleimidohexanoyl chloride **2b** (yield> 99%): ^{1}H NMR (400 MHz, $CDCl_3$, δ): 1.26 (m, -C**H$_2$**CH$_2$CH$_2$COCl-, 2H), 1.52 (quint, -C**H$_2$**CH$_2$COCl, 2H), 1.64 (quint, -NCH$_2$C**H$_2$**-, 2H), 2.82 (t, $^3J_{H-H}$ = 7.6 Hz, -C**H$_2$**COOH, 2H), 3.42 (t, $^3J_{H-H}$ = 7.33 Hz, -NC**H$_2$**-, 2H), 6.63 (s, -C**H**=C**H**-, 2H). ^{13}C NMR (101 MHz, $CDCl_3$, δ): 24.1 (s, -**C**H$_2$CH$_2$COOH-), 26.1 (s, -NCH$_2$CH$_2$**C**H$_2$-), 28.2 (s, -NCH$_2$**C**H$_2$-), 33.8 (s, -**C**H$_2$COOH-), 37.6 (s, -N**C**H$_2$-), 134.1 (s, -CO**C**H=**C**H-), 170.9 (s, -**C**ON-), 179.7 (s, -CH$_2$**C**OOH).

11-maleimidoundecanoyl chloride **2c** (yield>99 %): ^{1}H NMR (400MHz, C_6D_6, δ): 1.47-1.51 (m, N-CH$_2$CH$_2$(C**H$_2$**)$_6$CH$_2$CH$_2$(CO)-, 12H), 1.76 (p, N-CH$_2$C**H$_2$**(CH$_2$)$_6$-, $^3J_{H-H}$=6.6 Hz, 2H), 1.90 (p, Cl(CO)-CH$_2$C**H$_2$**(CH$_2$)$_6$-, 2H), 3.12 (t, Cl(CO)C**H$_2$**-, $^3J_{H-H}$=7.2 Hz, 2H), 3.67 (t, -N-C**H$_2$**-, $^3J_{H-H}$=7.2 Hz, 2H), 6.90 (s, -(CO)-C**H**=C**H**-(CO)-, 2H). ^{13}C NMR (101 MHz, C_6D_6, δ): 24.8 (s, -NCH$_2$**C**H$_2$-), 28.1 (s, -**C**H$_2$CH$_2$COOH-), 29.2 N-

$CH_2CH_2(\mathbf{C}H_2)_6CH_2CH_2(CO)$-, 33.9 (s, -N**C**$H_2$-), 37.5 (s, -**C**$H_2$COOH-), 134.0 (s, -CO**C**H=**C**H-), 172.0 (s, -**C**ON-), 179.9 (s, -CH_2**C**OOH).

Syntheses of maleimide poly(HFPO) M_w~1250 g/mol

To a mixture of oligo(HFPO) methylene alcohol and dry triethylamine (1.5 eq) in dry DCM, a solution of the corresponding maleimido acid chloride (1 eq) in dry DCM was added dropwise. The mixture was then heated under reflux during 1 h. The volatiles were then removed under reduced pressure. The product was diluted in 1,1,1,3,3-pentafluorobutane and washed three times with D.I. water. After the removal of 1,1,1,3,3-pentafluorobutane, the product was filtrated through a 1.2 µm filter frit before photopolymerization.

M1 C5 **3b** (yield=91 %): ^{1}H NMR (400 MHz, C_6D_6, δ): 1.46 (p, $^3J_{H-H}$ = 7.4 Hz, -$N(CH_2)_2C\mathbf{H}_2(CH_2)_2C(O)O$-, 2H), 1.72 (p, $^3J_{H-H}$ = 7.4 Hz, -$NCH_2C\mathbf{H}_2$-, 2H), 1.81 (p, $^3J_{H-H}$ = 7.38 Hz, $N(CH_2)_3C\mathbf{H}_2CH_2C(O)O$-, 2H), 2.50 (t, $^3J_{H-H}$ = 7.4 Hz, -C**H**$_2$CO-, 2H), 3.61 (t, $^3J_{H-H}$ = 7.4 Hz, -NC**H**$_2$-, 2H), 4.79 (dd, $^2J_{H-H}$ = 30.3 Hz, -, $^3J_{H-F}$ = 12.9 Hz, -$CF(CF_3)C\mathbf{H}_2O$-, 1H), 4.83 (dd, $^2J_{H-H}$ = 30.3 Hz, -, $^3J_{H-F}$ = 12.9 Hz, -$CF(CF_3)C\mathbf{H}_2O$-, 1H), 6.90 (s, -C(O)C**H**=C**H**C(O)-, 2H) ^{13}C NMR (101 MHz, C_6D_6, δ): 23.7 (s, -C(O)$CH_2\mathbf{C}H_2$-), 25.7 (s, -C(O)$CH_2CH_2\mathbf{C}H_2$-), 27.9 (s, -$NCH_2\mathbf{CH_2}$-), 32.7 (s, -C(O)**C**H_2), 36.8 (s, -N**C**H_2-), 59.0 (d, $^2J_{C-F}$ = 32.7 Hz, -$CF(CF_3)\mathbf{C}H_2O$-), 133.6 (s, -C(O)**C**H=**C**HC(O)-), 170.0 (s, -**C**(O)CH=CH**C**(O)-), 170.6 (s, -O**C**(O)-) ^{19}F NMR (376 MHz, C_6D_6, δ): = -134.6 $R_fC\mathbf{F_2}(CF_3)CH_2O(CO)R_h$, GC-MS, 70 eV, *m/z*: 41.1 (13), 54.05 (10), 55.1 (24), 68.05 (12), 69.05 (65), 82.05 (18), 83.1 (13), 97.1 (31), 98.05 (26), 110.05 (100), 111.05 (23), 112.1 (12), 147 (14), 150.05 (13), 169 (45), 193.05 (22), 194.05 (54), FT-IR (ATR) ν_{max} (cm^{-1}): 827.5 – 980.3 – 1119.0 – 1227.7 – 1709.8

M1 C10 **3c** (yield=95 %): ^{1}H NMR (400 MHz, C_6D_6, δ): 1.45 m, -$N(CH_2)_2(C\mathbf{H}_2)_6CH_2$-, 12H), 1.71 (p, $^3J_{H-H}$ = 7.2 Hz, -$NCH_2C\mathbf{H}_2$-, 2H), 1.78 (p, $^3J_{H-H}$ = 7.2 Hz, $N(CH_2)_8C\mathbf{H}_2CH_2C(O)O$-, 2H), 2.48 (t, $^3J_{H-H}$ = 7.2 Hz, -$CH_2C\mathbf{H}_2C(O)O$-, 2H), 3.61 (t, $^3J_{H-H}$ = 7.2 Hz, -NC**H**$_2$-, 2H), 4.76 (dd, $^2J_{H-H}$ = 30.3 Hz, $^3J_{H-F}$ = 12.9 Hz, -$CF(CF_3)C\mathbf{H}_2O$-, 1H), 4.79 (dd, $^2J_{H-H}$ = 30.3 Hz, $^3J_{H-F}$ = 12.9 Hz, -$CF(CF_3)C\mathbf{H}_2O$-, 1H), 6.69 (s, -C(O)C**H**=C**H**C(O)-, 2H). ^{13}C NMR (101 MHz, C_6D_6, δ): 24.5 (s, -C(O)$CH_2\mathbf{C}H_2$-), 26.7 (s, -$NCH_2\mathbf{CH_2}$-), 28.5 (s, -**C**H_2-), 29.0 (s, -**C**H_2-), 29.1 (s, -**C**H_2-), 29.2 (s, -**C**H_2-), 29.36 (s, -**C**H_2-), 29.44 (s, -**C**H_2-), 59.1 (d, $^2J_{C-F}$ = 32.7 Hz, -$CF(CF_3)\mathbf{C}H_2O$-), 133.5 (-C(O)**C**H=**C**HC(O)-), 170.0 (s, -**C**(O)CH=CH**C**(O)-), 170.6 (s, -O**C**(O)-). ^{19}F NMR (376 MHz, C_6D_6, δ): -134.4 $R_fC\mathbf{F_2}(CF_3)CH_2O(CO)R_h$ GC-MS, 70 eV, *m/z*: 41.1 (24), 55.1 (53), 69.05 (82), 81,1 (27), 82.05 (28), 83.1 (40), 97,1 (24), 98.05 (34), 100.05 (18), 110.05 (100), 111.05 (45), 119.05 (13), 147.1 (28), 149.15 (31), 150.05 (14), 169 (45), 191.15 (13), 263.15 (43), 264.15 (89), FT-IR (ATR) ν_{max} (cm^{-1}): 827.4 – 980.7 – 1119.8 – 1228.4 – 1708.8

Syntheses of maleimide poly(HFPO) M_w~2000 g/mol

To a solution of oligo(HFPO) methylene alcohol (M_w=2000 g/mol, 2 g, 1 mmol), the corresponding maleimide (2 eq) and DMAP (0.1 eq) in 1,1,1,3,3-pentafluorobutane (15 mL), 2.2eq of DCC in DCM (10 mL) were added dropwise at 0°C during 30 min. After 5 min of reaction, the ice bath was removed. The conversion of the reaction was followed by ^{19}F NMR. After 30 min, the reaction was stopped. The reaction mixture was filtrated and concentrated under vacuum. Flash column chromatography by solid deposit with silica was performed (15:95 EtOAc:Pentane). The solvents were removed under vacuum to afford white blurry oils.

M2 C3 **4a** (yield=69 %): ^{1}H NMR (400 MHz, C_6D_6, δ): 1.81 (br, -$NCH_2C\mathbf{H}_2CH_2$-, 2H), 2.34 (br, -$CH_2C\mathbf{H_2}C(O)O$-, 2H), 3.47 (br, -NC**H**$_2$-, 2H), 4.66 (m, $^2J_{H-H}$ = 34.6 Hz, $^3J_{H-F}$ = 12.1 Hz, -$CF(CF_3)C\mathbf{H_2}O$-, 2H), 6.63 (br, -C(O)C**H**=C**H**C(O)-, 2H) ^{13}C NMR (101 MHz, C_6D_6, δ): 22.4 (-$NCH_2\mathbf{C}H_2CH_2$-), 30.2 (-$CH_2\mathbf{C}H_2C(O)O$-), 36.4 (-N**C**H_2-), 59.4 ($^2J_{C-F}$ = 31.4 Hz, -$CF(CF_3)\mathbf{C}H_2O$-), 134.0 (-C(O)**C**H=**C**HC(O)-), 170.7 (-**C**(O)CH=CH**C**(O)-), 170.8 (-$CF(CF_3)CH_2O(\mathbf{C}O)$-) ^{19}F NMR (376 MHz, C_6D_6, δ): -134.3 $R_fC\mathbf{F_2}(CF_3)CH_2O(CO)R_h$ GC-MS, 70 eV, *m/z*: 69.1 (37), 82.1 (15), 100 (14), 110.1 (51), 119

(13), 124.1 (14), 137.1 (16), 138.1 (23), 147 (24), 150 (28), 165.1 (18), 166.1 (76), 169 (100), 335 (18), 528.2 (14) MALDI-TOF, $[M+Li]^+$: 1818.6 – 1984.8 – 2151.0 – 2316.3 – 2482.5 FT-IR (ATR) ν_{max} (cm^{-1}): 828.0 – 982.4 – 1126.3 – 1232.4 – 1715.7

M2 C5 **4b** (yield=84 %): ^{1}H NMR (400 MHz, C_6D_6, δ): 1.28 (br, -N(CH_2)$_2$(C**H$_2$**)CH_2-, 2H), 1.54 (br, -NCH_2C**H$_2$**-, 2H), 1.62 (br, N(CH_2)$_8$C**H$_2$**CH_2C(O)O-, 2H), 2.34 (br, -CH_2C**H$_2$**C(O)O-, 2H), 3.43 (br, -NC**H$_2$**-, 2H), 4.69 (m, $^2J_{H-H}$ = 31.4 Hz, $^3J_{H-F}$ = 12.8 Hz, -CF(CF_3)C**H$_2$**O-, 2H), 6.67 (br, -C(O)C**H**=C**H**C(O)-, 2H) ^{13}C NMR (101 MHz, C_6D_6, δ): 23.9 (NCH_2(CH_2)$_2$**C**$H_2$$CH_2$C(O)O-), 25.9 (-N$CH_2$**C**$H_2$-), 28.0 (-N($CH_2$)$_2$(**C**$H_2$)$CH_2$-), 32.8 (-$CH_2$**C**$H_2$C(O)O-), 37.1 (-N**C**$H_2$-), 59.2 ($^2J_{C-F}$ = 30.4 Hz, -CF(CF_3)**C**H_2O-), 134.0 (-C(O)**C**H=**C**HC(O)-), 170.6 (-**C**(O)CH=CH**C**(O)-), 171.1 (-CF(CF_3)CH_2O(**C**O)-) ^{19}F NMR (376 MHz, C_6D_6, δ): -134.9 R_fC**F$_2$**(CF_3)CH_2O(CO)R_h GC-MS, 70 eV, *m/z*: 54(10), 55 (12), 69.2 (37), 82.2 (15), 100 (21), 110 (100), 111 (16), 147 (16), 150 (31), 169 (88), 193.1 (15), 194.1 (32), 335.1 (16) MALDI-TOF, $[M+Li]^+$: 1846.6 – 2012.8 – 2179.1 – 2344.3 – 2510.5 FT-IR (ATR) ν_{max} (cm^{-1}): 827.0 – 978.9 – 1117.4 – 1226.9 – 1711.6

M2 C10 **4c** (yield=86 %): ^{1}H NMR (400 MHz, C_6D_6, 50 °C, δ): 1.22 (m, -N(CH_2)$_2$(C**H$_2$**)$_6$$CH_2$-, 12H), 1.49 (br, -NC$H_2$C**H$_2$**-, 2H), 1.56 (br, N($CH_2$)$_8$C**H$_2$**$CH_2$C(O)O-, 2H), 2.29 (br, -$CH_2$C**H$_2$**C(O)O-, 2H), 3.39 (br, -NC**H$_2$**-, 2H), 4.60 (m, $^2J_{H-H}$ = 34.6 Hz, $^3J_{H-F}$ = 12.3 Hz,-CF(CF_3)C**H$_2$**O-, 2H), 6.61 (br, -C(O)C**H**=C**H**C(O)-, 2H) ^{13}C NMR (100 MHz, C_6D_6, δ): 24.5 (N(CH_2)$_6$**C**$H_2$$CH_2$C(O)O-), 26.9 (-N$CH_2$**C**$H_2$-), 28.7-29.6 (-N($CH_2$)$_2$(**C**$H_2$)$_6$$CH_2$-), 33.0 (-$CH_2$**C**$H_2$C(O)O-), 37.6 (-N**C**$H_2$-), 59.2 ($^2J_{C-F}$ = 30.5 Hz, -CF(CF_3)**C**H_2O-), 134.2 (-C(O)**C**H=**C**HC(O)-), 170.7 (-**C**(O)CH=CH**C**(O)-), 171.0 (-CF(CF_3)CH_2O(**C**O)-) ^{19}F NMR (376 MHz, C_6D_6, δ): -135.0 R_fC**F$_2$**(CF_3)CH_2O(CO)R_h GC-MS, 70 eV, *m/z*: 54.9 (11), 69 (53), 82 (24), 83.1 (12), 100 (26), 110 (100), 111 (16), 119 (16), 147 (16), 150.1 (32), 169.1 (87), 191.1 (14), 263.1 (30), 264.3 (46), 335 (19) MALDI-TOF, $[M+Li]^+$: 1917.0 – 2083.2 – 2249.5 – 2414.7 – 2581.0 FT-IR (ATR) ν_{max} (cm^{-1}): 826.9 – 979.1 – 1117.6 – 1227.1 – 1710.6

RESULTS AND DISCUSSION

Synthesis of the maleimide PFPAEs

Five different maleimides were synthesized according to Scheme 2 and their structures are depicted in Figure 1: they are characterized by PFPAE chains of different lengths (n=6.5 for M_x=M1 and n=11 for M_x=M2) and by a different spacer of 3, 5, 10- methylene units (-CH_2- unit) between the fluorinated chain and the maleimide group. The products will be named M_x C3, M_x C5, M_x C10 respectively.

The starting materials employed are two different oligo(HFPO) methylene alcohols M_x having a molecular weights of 1250 g/mol (n=6.5) and 2000 g/mol (n=11) labelled M1 and M2 respectively. The shortest molecular weight (i.e. 1250 g/mol) comes from the reduction of Krytox® acyl fluoride from Chemours Company whereas the longer molecular weight Krytox® Methylene Alcohol (i.e. 2000 g/mol) was directly provided by Chemours Company.

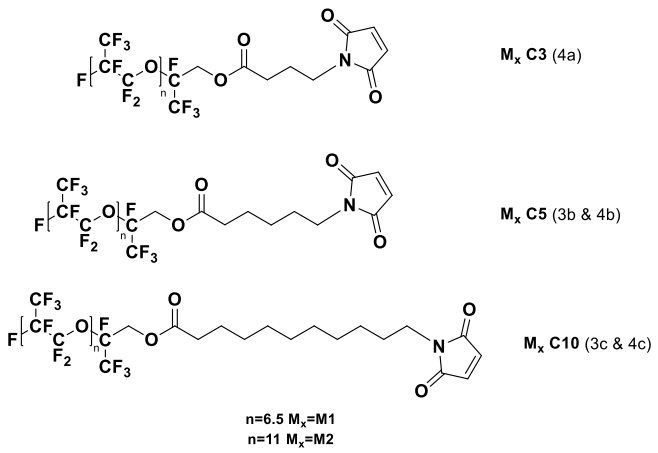
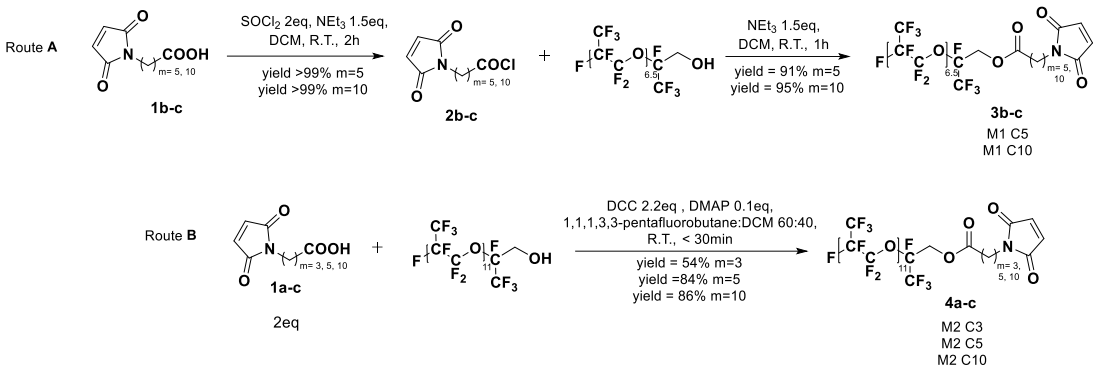


Figure 1: Structures of the different maleimide PFPAEs

In this work, the synthesis of PFPAEs maleimides was performed via a two-step or three-step reaction. The maleimides which were used were either commercial products (**1c**) or synthesized maleimides (**1a-b**) (see experimental section). Two different esterification methods were used.



Scheme 2 : Reaction scheme of the addition of maleimide groups to fluorinated oligomers

Macromonomers **3b-c** were efficiently synthesized via nucleophilic acyl substitution of the oligo(HFPO) alcohol M1 with the corresponding acyl chlorides (**2b-c**; the chlorinated analogues of **1b-c**) (Scheme 2. Route A.). However, **4a-c** (containing longer fluorinated chains) did not reach complete conversion by Route A. Previous work has shown Steglich esterification to provide a facile route for oligo(HFPO) methylene alcohol esterification, and this method enabled the successful synthesis of **4a-c** (Route B).[31]

According to thermal analysis, the maleimide functionalized PFPAE macromonomers exhibited improved thermal stability to the corresponding starting PFPAE alcohol. For example, Krytox® Methylene Alcohol M_w~1250 g/mol had a $T_{5\%}$ of 122 °C. With the substituents C5 and C10 added to the methylene alcohol, the $T_{5\%}$ was increased up to 200 °C for both products. For Krytox® Methylene Alcohol M_w~2000g/mol, the $T_{5\%}$ was increased from 200 °C for the starting alcohol to 233 °C, 248 °C and 253 °C for M2 C3, M2 C5 and M2 C10 respectively. However, the maleimide was expected to polymerize before degradation explaining the two different steps by TGA. The derivative highlights the presence of two distinct peaks which means two steps of degradation (Figure 2).

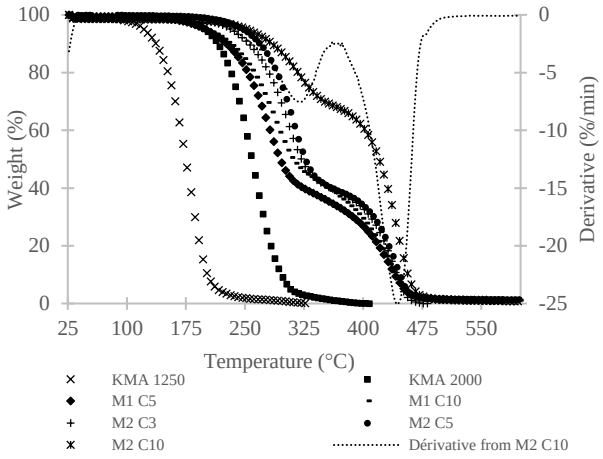


Figure 2: TGA curves of the starting Krytox® Methylene Alcohol (KMA) and the monomers M1 C5, M1 C10, M2 C3, M2 C5 and M2 C10 under nitrogen

In order to determine the phenomena that give rise to these two degradation peaks, thermogravimetric analysis coupled with infrared spectroscopy (TGA-IR) was used to identify the degradation products. The information provided by Figure 3 is the disappearance of the maleimide C=C bond (sp^2 C-H bending) at 826 cm^{-1} during the second degradation step. Thus, it implies that the first degradation pathway was the loss of the monomer with the presence of a band at 826 cm^{-1}. Next, the heat transfer from the TGA causes additional polymerization of the maleimide with no substantial weight loss, and finally the second degradation is evident as the maleimide polymer deteriorates.

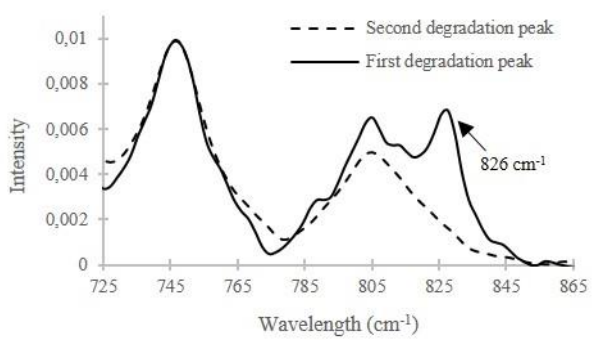


Figure 3: IR spectra of the degradation products during the first and second degradation steps

Kinetics studies of maleimide PFPAEs

The new maleimides were used as reactive monomers in photopolymerization. Photopolymerization kinetics were monitored by Real Time-FTIR. The effect of structural parameters was first studied and discussed depending on their photopolymerization kinetics. Then the photopolymerization conditions such as the presence of air and photoinitiator will be discussed.

Influence of the molecular weight of the PFPAE chain (M1-M2)

For the same hydrogenated spacer C5, two different products with two PFPAE chains were tested: M1 C5 and M2 C5. The conversion over time was calculated by measuring the decrease of the C=C band (sp^2 C-H bending) at 826 cm^{-1} until quantitative conversions of the products was evident. At 696 cm^{-1}, the C=C band loss also confirmed its complete disappearance (see Supporting Information). The higher molecular weight monomer (M2 C5) reached quantitative conversion in 10s, while the lower molecular weight monomer (M1 C5) reached only 17% conversion in the same period of time (Figure 4). Longer UV-curing time was required for M1 C5 to get to quantitative conversion (70 s). The assumption for the faster conversion rates is due to the higher percentage of fluorine. As fluorine content increases, there is larger amount of submicron segregation between the hydrogenated and fluorinated chains. Thus it promotes the increased probability of hydrogenated segments encountering each other for polymerization.

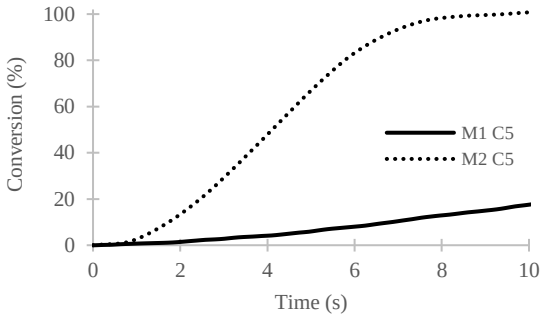


Figure 4: Photopolymerization conversion curves of M1 C5 and M2 C5 without air

Influence of the hydrogenated spacer and air on maleimide oligo(HFPO) M1

When the homopolymerization of the maleimide monomers M1 C5 and M1 C10 were performed in the absence of air as shown on Figure 5, both monomers achieved quantitative conversion by 70 s. They both reached roughly 95% conversion in 40 s. However, M1 C10 exhibited a greater initial rate of polymerization than M1 C5, which could be due to the increased flexibility of the longer hydrogenated spacer C10. A higher flexibility could help to facilitate the submicron segregation and then increase the proximity of the hydrogenated maleimides.

Maleimides are known to demonstrate less oxygen inhibition than (meth)acrylate systems.[32] Indeed, both monomers, M1 C5 and M1 C10, achieved complete conversion in the absence and in the presence of air (Figure 5). However, oxygen inhibition was observed. M1 C5 demonstrated a higher oxygen inhibition as a complete conversion was obtained after more than 400 s under air. On the contrary, M1 C10 showed a complete conversion in less than 150 s under air. Consequently, the difference between both hydrogenated spacers C5 and C10 was more visible in the presence of air. Moreover, longer aliphatic chains for common organic solvents (i.e. heptane and octane) displayed lower solubility in oxygen than the shorter alkanes (i.e. pentane and hexane).[33] Therefore, the lower solubility of M1 C10 with oxygen could

explain the shorter inhibition step and the faster reaction in comparison to the shorter M1 C5.

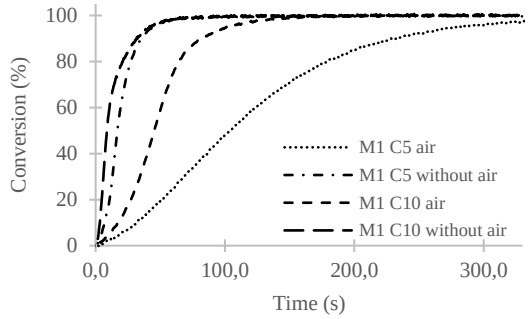


Figure 5: Photopolymerization conversion curves for M1 C5 and M1 C10 with and without air

Influence of the hydrogenated spacer and air on maleimide oligo(HFPO) M2

In comparison to the lower molecular weight (M1 products), the hydrogenated spacer was not a key factor for the reaction speed for M2 products due to the longer HFPO segment. A complete conversion was reached after 8 s without air and after 40 s in the presence of air (Figure 6). Oxygen inhibition was observed at the beginning until 10 s and then the reaction speed increased (Figure 6). Nonetheless, all M2 products reached the quantitative conversion at the same time in comparison to M1 products.

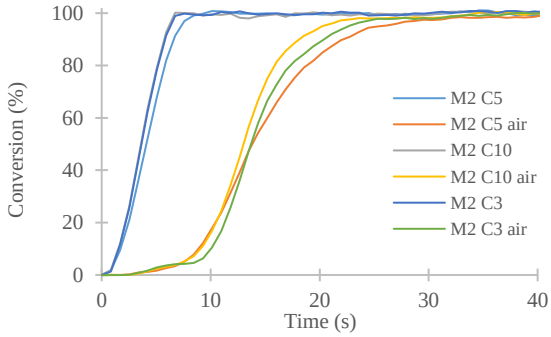


Figure 6 : Photopolymerization conversion curves for M2 C3, C5 and C10 with and without of air

Influence of the presence of photoinitiator

As mentioned earlier, maleimides can polymerise without photoinitiators. However, it seems interesting to evaluate the effect of the photoinitiator on the photopolymerization processes without air and M2 C10 was chosen as the reference. Three different Norrish II-type photoinitiators were used: phenylbis(2,4,6-trimethylbenzoyl)phosphine oxide (BAPO), diphenyl(2,4,6-trimethylbenzoyl)phosphine oxide (TPO) and 2-hydroxy-2-methylpropiophenone (Darocur 1173). The photoinitiator efficiency follows this order: TPO>BAPO>Darocur (Figure 7). Only TPO permitted faster photopolymerization kinetics than the maleimide on its own (Table 1). Having a photoinitiator seemed to increase the speed reaction during the first seconds but after 80 % - 90 % of conversion, the reaction speed slowed down. Therefore, the declining rates seem to differ between the reactions with and without photoinitiators. However, in 15 s, a quantitative conversion was obtained for the pure M2 C10, TPO and BAPO. Darocur 1173 showed the lowest solubility by forming a gel with M2 C10 which could explain the slower conversion.

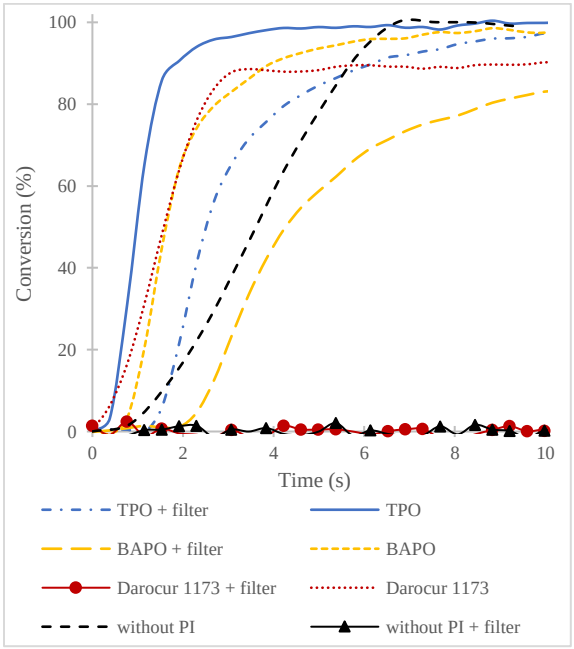


Figure 7: Photopolymerization curves for the use of different photoinitiators (2% w/w) and a cut-off filter

A cut-off filter was also employed (irradiation area: 400-500 nm) for some experiments to avoid absorption of light by the maleimide[32] and to induce initiation exclusively by the photoinitiator. The aim of the filter was to separate the initiating and the propagation steps. Two initiators were effective in this zone:

BAPO and TPO due to an absorption between 400-500 nm. In contrary, Darocur 1173 does not absorb in this zone. Consequently, in the presence of a filter, no conversion was noted for the pure product as well as with Darocur 1173 (Table 1). Nonetheless, TPO showed a faster conversion than BAPO. Moreover, in the presence of a filter, an inhibition step was detected at the beginning. Therefore, the initiating step appeared to last 1.5s and 2s for TPO and BAPO respectively and then the reactions went until complete conversion in 17 s for TPO and in 50 s for BAPO (Table 1). In any case, the use of photoinitiator was not essential as the difference between no photoinitiator and TPO is very slight to reach the quantitative conversion: 8 s versus 5 s in the absence of photoinitiator.

Table 1: Table of the experimental conditions with and without photoinitiators (2% w/w)

Sample	Inhibition delay (s)	Quantitative conversion time (s)	Conversion rate at 10s (%)
Without PI	> 1	8	100
Without PI + filter	--	No conversion	0
TPO	> 0.5	5	100
TPO + filter	1.5	17	97
BAPO	> 1	15	97.5
BAPO + filter	2	50	83
Darocur 1173	0	130	90
Darocur 1173+ filter	--	No conversion	0

Thermal and surface properties

The starting monomers as well as the cured polymers were analyzed by TGA and DSC. Contact angle measurements were also performed by using distilled water and hexadecane.

Thermogravimetric analyses (TGA)

The different maleimides were tested by TGA to study their thermal behaviour.

The homopolymers M1 C5 and M1 C10 exhibited a $T_{5\%}$ of 230 °C. The difference in hydrocarbon chain lengths did not show any substantial improvement for the $T_{5\%}$. The only noticeable difference is that M1 C10's degradation kinetics are slower (monomer and homopolymer). For the highest molecular weight oligo(HFPO) M2 series, the $T_{5\%}$ temperatures were 306 °C, 323 °C and 336 °C for M2 C3, M2 C5 and M2 C10 respectively. All displayed better thermal stability than their corresponding monomers (Figure 8).

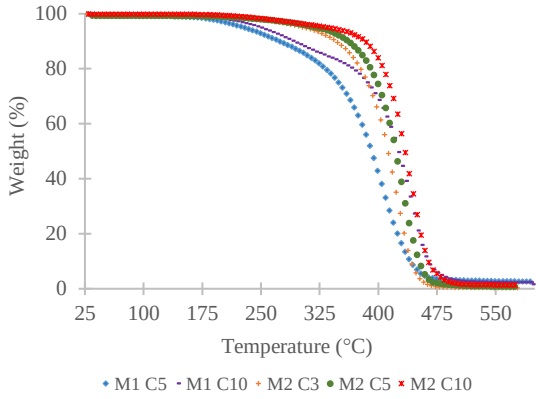


Figure 8: TGA curves of polymers after UV-curing under nitrogen

These degradation temperatures demonstrate a good thermal resistance in comparison to a previous study about the copolymers (maleate-*alt*-vinyl ether) PFPAEs.[31] The most thermally stable homopolymer M2 C10 ($T_{10\%}$ - 10 K/min: 360 °C in N_2 and 92 °C in air – Figure 9) showed higher thermal stability than cross-linked PFPAEs with acrylate bonds ($T_{10\%}$ - N_2 = 256 °C – 280 °C).[34] They were also comparable to materials based on stronger triazole bonds under air ($T_{10\%}$ = 305 °C and 336 °C) containing PFPAEs and perfluoroalkyl chains.[35] However, the maleimides obviously showed a faster degradation kinetic in presence of air and seemed to be more sensitive to oxidation degradation even if these non-crosslinked polymers provided good results in terms of thermal stability.

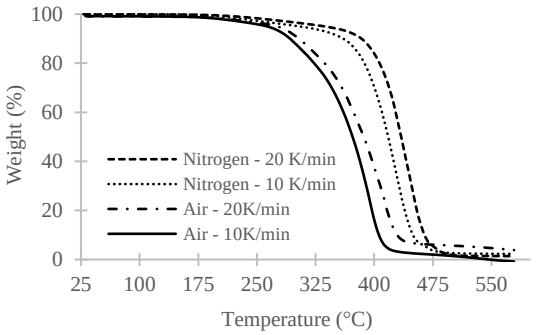


Figure 9: TGA curves of UV-cured M2C10 under nitrogen and air at different heating rates

Differential Scanning Calorimetry analyses

The glass transition temperatures of the different homopolymers were also studied. They showed very similar values from -71 °C to -66°C for the homopolymers. In any case, only the glass transition temperatures of the fluorinated phase were detected. Indeed, as it is a branched homopolymer containing many fluorinated units for each maleimide unit, it overlapped the effect of the hydrogenated counterpart from the maleimide groups. Another observation concerns the $T_{melting}$ for only one of the experimental monomers, M2 C10. The melting point ($T_{melting}$) for this monomer was -23 °C. This is due to the long aliphatic chain of C10 and has a comparable melting point to decane, $T_{melting}$= -29.7 °C. However, surprisingly, no melting temperature was observed for M1 C10 (see supporting information)

Contact angle measurements

After spin-coating the maleimide PFPAEs onto glass slides and photopolymerizing them using a conveyor bench, the contact angles of the products were examined.

Table 2: Contact angle values for water and hexadecane

Contact angle (°)	M1 C5	M1 C10	M2 C3	M2 C5	M2 C10
Water	113	117	99	104	124
Hexadecane	76	78	66	67	82

The polymers revealed hydrophobic and oleophobic properties (Table 2). In this study, the contact angles were dependent on the chain flexibility afforded by the hydrogenated spacer. The longer the spacer the better flexibility and consequently, the better segregation permitted. These attributes lead to higher contact angle values. It was assumed that the segregation occurred due to the glass support and altered the contact angles. It has already been reported for cross-linked methacrylate PFPAEs with different contact angles between the air and the glass sides.[36,37] Moreover, the values are in good agreement with previous values found for methacrylate PFPAEs homopolymers[38] or cross-linked acrylates PFPAEs.[34,39] By using hexadecane, the same trend was observed: an increase of the hydrogenated spacer length permitted an increase in contact angle values. The omniphobic properties were then proved and the polymers can be used for water-oil repellent applications.

CONCLUSIONS

Maleimide groups bonded to PFPAEs allowed for very rapid polymerization under UV-light without photoinitiator. The effect of molecular weight of the oligo(HFPO) was most significant. Longer fluorinated chains permitted increased segregation of the hydrocarbon and fluorocarbon portions of the polymer. This higher degree of segregation increased the rate of polymerization. Moreover, the effect of the hydrogenated spacer was then hidden by the highest molecular weight HFPO chain. The presence of air showed a slight influence in comparison to some acrylic systems. Indeed, even if oxygen inhibition was observed at the beginning, complete conversion was easily obtained. Excellent thermal and omniphobic properties were also exhibited by these homopolymers and far superior to cross-linked acrylate PFPAEs materials previously used in microfluidics.

ACKNOWLEDGEMENTS

This research project has received funding from the European Union's Horizon 2020 research and innovation program under grant agreement No. 690917 – PhotoFluo; Natural Sciences and Engineering Research Council of Canada (NSERC), Discovery Grants Program RGPIN-2015-05513 and Ministère de l'Enseignement Supérieure et de la Recherche.

REFERENCES AND NOTES

(1) Oster, G.; Yang, N. L. *Chem. Rev.* **1968**, *68* (2), 125.

(2) von Sonntag, J.; Beckert, D.; Knolle, W.; Mehnert, R. *Radiat. Phys. Chem.* **1999**, *55* (5–6), 609.

(3) von Sonntag, J.; Knolle, W. *J. Photochem. Photobiol. A Chem.* **2000**, *136* (1–2), 133.

(4) Vázquez, C. P.; Joly-Duhamel, C.; Boutevin, B. *Macromol. Chem. Phys.* **2009**, *210* (3–4), 269.

(5) Hoyle, C. E.; Clark, S. C.; Jonsson, S.; Shimose, M. *Polymer (Guildf).* **1997**, *38* (22), 5695.

(6) Jönsson, S.; Sundell, P. E.; Shimose, M.; Clark, S.; Miller, C.; Morel, F.; Decker, C.; Hoyle, C. E. *Nucl. Instruments Methods Phys. Res. Sect. B Beam Interact. with Mater. Atoms* **1997**, *131* (1–4), 276.

(7) Pozos vázquez, C.; Tayouo, R.; Joly-Duhamel, C.; Boutevin, B. *J. Polym. Sci. Part A Polym. Chem.* **2010**, *48* (10), 2123.

(8) Ahn, K.-D.; Kang, J.-H.; Yoo, K. W.; Choo, D. J. *Macromol. Symp.* **2007**, *254* (1), 46.

(9) Dolci, E.; Froidevaux, V.; Joly-Duhamel, C.; Auvergne, R.; Boutevin, B.; Caillol, S. *Polym. Rev.* **2016**, *56* (3), 512.

(10) Barrales-Rienda, J. M.; Ramos, J. G.; Chavez, M. S. *J. Fluor. Chem.* **1977**, *9* (4), 293.

(11) Barrales-Rienda, J. M.; Ramos, J. G.; Chaves, M. S. *J. Polym. Sci. Polym. Chem. Ed.* **1979**, *17* (1), 81.

(12) Mokhtar, S. M.; Abd-Elaziz, S. M.; Gomaa, F. A. *J. Fluor. Chem.* **2010**, *131* (5), 616.

(13) Hendlinger, P.; Laschewsky, A.; Bertrand, P.; Delcorte, A.; Legras, R.; Nysten, B.; Möbius, D. *Langmuir* **1997**, *13* (2), 310.

(14) Jain, D.; Maheshwari, J.; Rathore, N.; Paliwal, S. N. *Rasayan J. Chem.* **2012**, *5* (4), 445.

(15) Daukiya, L.; Mattioli, C.; Aubel, D.; Hajjar-Garreau, S.; Vonau, F.; Denys, E.; Reiter, G.; Fransson, J.; Perrin, E.; Bocquet, M. L.; Bena, C.; Gourdon, A.; Simon, L. *ACS Nano* **2017**, *11* (1), 627.

(16) Beaune, O.; Bessière, J. M.; Boutevin, B.; Robin, J. J. *J. Fluor. Chem.* **1994**, *67* (2), 159.

(17) Boutevin, B.; Lusinchi, J. M.; Pietrasanta, Y.; Robin, J. J. *J. Fluor. Chem.* **1995**, *73* (1), 79.

(18) Soules, A.; Pozos Vázquez, C.; Améduri, B.; Joly-Duhamel, C.; Essahli, M.; Boutevin, B. *J. Polym. Sci. Part A Polym. Chem.* **2008**, *46* (10), 3214.

(19) Cummings, W.; Lynch, E. R. Polyimides. GB1077243A, 1965.

(20) Green, H. E.; Jones, R. J.; O'Rell, M. K. Bis di(fluoromaleimide) capped polymers. 4,173,700, 1989.

(21) Shiue, C.-Y.; Wolf, A. P.; Hainfeld, J. F. *J. Label. Compd. Radiopharm.* **1989**, *26* (1–12), 287.

(22) De Bruin, B.; Kuhnast, B.; Hinnen, F.; Yaouancq, L.; Amessou, M.; Johannes, L.; Samson, A.; Boisgard, R.; Tavitian, B.; Dollé, F. *Bioconjug. Chem.* **2005**, *16* (2), 406.

(23) Fujita, Y.; Murakami, Y.; Noda, A.; Miyoshi, S. *Bioconjug. Chem.* **2017**, *28* (2), 642.

(24) Berndt, M.; Pietzsch, J.; Wuest, F. *Nucl. Med. Biol.* **2007**, *34* (1), 5.

(25) Dollé, F.; Hinnen, F.; Lagnel, B.; Boisgard, R.; Sanson, A.; Russo-Marie, F.; Tavitian, B. *J. Label. Compd. Radiopharm.* **2003**, *46* (S1), S15.

(26) Cai, W.; Zhang, X.; Wu, Y.; Chen, X. *J Nucl Med* **2006**, *47* (7), 1172.

(27) Ameduri, B.; Boutevin, B.; Ameduri, B.; Boutevin, B. In *Well-Architectured Fluoropolymers: Synthesis, Properties and Applications*; 2004; pp 187–230.

(28) Malinverno, G.; Pantini, G.; Bootman, J. *Food Chem. Toxicol.* **1996**, *34* (7), 639.

(29) Pantini, G. *Clin. Dermatol.* **2008**, *26* (4), 387.

(30) Zhang, C.; Moonshi, S. S.; Wang, W.; Ta, H. T.; Han, Y.; Han, F. Y.; Peng, H.; Král, P.; Rolfe, B. E.; Gooding, J. J.; Gaus, K.; Whittaker, A. K. *ACS Nano* **2018**, *12* (9), 9162.

(31) Bonneaud, C.; Decostanzi, M.; Burgess, J.; Trusiano, G.; Burgess, T.; Bongiovanni, R.; Joly-Duhamel, C.; Friesen, C. M. *RSC Adv.* **2018**, *8* (57), 32664.

(32) Decker, C.; Bianchi, C.; Morel, F.; Jönsson, S.; Hoyle, C. *Macromol. Chem. Phys.* **2000**, *201* (13), 1493.

(33) Sato, T.; Hamada, Y.; Sumikawa, M.; Araki, S.; Yamamoto, H. *Ind. Eng. Chem. Res.* **2014**, *53* (49), 19331.

(34) Bongiovanni, R.; Medici, A.; Zompatori, A.; Garavaglia, S.; Tonelli, C. *Polym. Int.* **2012**, *61* (1), 65.

(35) Lopez, G.; Ameduri, B.; Habas, J. P. *Macromol. Rapid Commun.* **2016**, *37* (8), 711.

(36) Hu, Z.; Chen, L.; Betts, D. E.; Pandya, A.; Hillmyer, M. A.; DeSimone, J. M. *J. Am. Chem. Soc.* **2008**, *130* (43), 14244.

(37) Wang, Y.; Pitet, L. M.; Finlay, J. a.; Brewer, L. H.; Cone, G.; Betts, D. E.; Callow, M. E.; Callow, J. a.; Wendt, D. E.; Hillmyer, M. a.; DeSimone, J. M. *Biofouling* **2011**, *27* (10), 1139.

(38) Bongiovanni, R.; Di Meo, A.; Pollicino, A.; Priola, A.; Tonelli, C. *React. Funct. Polym.* **2008**, *68* (1), 189.

(39) Vitale, A.; Priola, A.; Tonelli, C.; Bongiovanni, R. *Polym. Int.* **2013**, *62* (9), 1395.

GRAPHICAL ABSTRACT

Céline Bonneaud[1], Julia M. Burgess[2], Roberta Bongiovanni[3], Christine Joly-Duhamel[1]* and Chadron M. Friesen[2]*

Photopolymerization of maleimide perfluoropolyalkylethers (PFPAEs) in the absence of photoinitiator

The polymerization under UV-light of maleimide PFPAEs is very fast. The example shown in the figure demonstrates a curing time of 8 s. After UV-curing, the maleimide PFPAEs reveal excellent thermal stability. Moreover, hydrophobicity and oleophobicity are exhibited with contact angle values up to 124° with water and up to 82° with hexadecane.

GRAPHICAL ABSTRACT FIGURE ((Please provide a square image to be produced at 50 mm wide by 50 mm high. Please avoid graphs and other figures with fine detail due to the relatively small size of this image.))

